RESEARCH ARTICLE

Staphylococcus aureus impairs dermal fibroblast functions with deleterious effects on wound healing

Masaya Yokota[1,2] | Nicola Häffner[3] | Matthew Kassier[1] | Matthias Brunner[1] |
Srikanth Mairpady Shambat[3] | Fabian Brennecke[1] | Janine Schniering[1] |
Ewerton Marques Maggio[4] | Oliver Distler[1] | Annelies Sophie Zinkernagel[3] | Britta Maurer[1,5]

[1]Center of Experimental Rheumatology, Department of Rheumatology, University Hospital Zurich, Zurich, Switzerland

[2]Department of Allergy and Clinical Immunology, Graduate School of Medicine, Chiba University, Chiba, Japan

[3]Department of Infectious Diseases and Hospital Epidemiology, University Hospital Zurich, University of Zurich, Zurich, Switzerland

[4]Institute of Pathology and Molecular Pathology, University Hospital Zurich, Zurich, Switzerland

[5]Department of Rheumatology and Immunology, University Hospital Bern, University Bern, Bern, Switzerland

Correspondence
Britta Maurer, Center of Experimental Rheumatology, Department of Rheumatology, Gloriastrasse 25, 8091 Zurich, Switzerland.
Email: Britta.Maurer@usz.ch

Funding information
Prof. Max Cloetta Foundation; Abbvie | AbbVie Deutschland (AbbVie Germany); Novartis Stiftung für Medizinisch-Biologische Forschung (Novartis Foundation for Medical-Biological Research); Olga Mayenfisch Foundation; Vontobel-Stiftung (Vontobel Foundation); EMDO Stiftung (EMDO-Stiftung); Herzog Egli Foundation; Schweizerischer Nationalfonds zur Förderung der Wissenschaftlichen Forschung (SNF), Grant/Award Number: 31003A_176252

Abstract

Chronic wounds are a major disease burden worldwide. The breach of the epithelial barrier facilitates transition of skin commensals to invasive facultative pathogens. Therefore, we investigated the potential effects of *Staphylococcus aureus* (SA) on dermal fibroblasts as key cells for tissue repair. In co-culture systems combining live or heat-killed SA with dermal fibroblasts derived from the BJ-5ta cell line, healthy individuals, and patients with systemic sclerosis, we assessed tissue repair including pro-inflammatory cytokines, matrix metalloproteases (MMPs), myofibroblast functions, and host defense responses. Only live SA induced the upregulation of IL-1β/-6/-8 and MMP1/3 as co-factors of tissue degradation. Additionally, the increased cell death reduced collagen production, proliferation, migration, and contractility, prerequisite mechanisms for wound closure. Intracellular SA triggered inflammatory and type I IFN responses via intracellular dsDNA sensor molecules and MyD88 and STING signaling pathways. In conclusion, live SA affected various key tissue repair functions of dermal fibroblasts from different sources to a similar extent. Thus, SA infection of dermal fibroblasts should be taken into account for future wound management strategies.

KEYWORDS
fibroblasts, staphyloccous aureus, wound healing

1 | INTRODUCTION

Chronic wounds have become a problem of epidemic proportions worldwide.[1,2] Disturbed circulation due to macroangiopathy as in peripheral arterial occlusive disease or resulting from microangiopathy such as in diabetes mellitus or certain autoimmune disorders is a major contributing factor.[3] For example in systemic sclerosis (SSc), a multi-systemic autoimmune connective tissue disease, up to two thirds of patients suffer from chronic digital ulcers (DU),[4] which are often complicated by necrosis, soft tissue infection, and osteomyelitis.[5] Chronic non-healing wounds are characterized by persistent inflammation, defective re-epithelialization, and impaired matrix remodeling.[3,6] Chronic wounds are always colonized by bacteria.[1,7] In dermal ulcers, the breach of the basement membrane[8] exposes dermal tissue and cells to commensal skin bacteria, facilitating invasion.[9] *Staphylococcus aureus* (SA) is a common colonizer of the human skin and one of the most prevalent opportunistic pathogens in chronic wounds[1,10,11] as well as a cause of serious local and systemic infections.[12] SA produces various virulent factors such as α-toxin, enterotoxins, and coagulase, which damage cell membranes and induce cell death.[13] In addition, cell surface molecules such as lipopeptides, peptidoglycan and lipoprotein can activate immune cells via pattern (=pathogen) recognition receptors (PRRs) resulting in an enhanced pro-inflammatory response, which also delays wound healing.[14] However, recent research points toward novel mechanisms of SA pathogenicity with respect to chronic and/or recurrent wound infections. While long considered a strictly extracellular pathogen, recent studies showed that SA survived phagocytosis by macrophages and neutrophils, and induced its intracellular uptake even in non-professional phagocytes including, for example, epithelial and endothelial cells, osteoblasts, and murine fibroblasts.[9,15] Intracellular SA causes cytotoxicity, but also may progress to persistence and then represents a mechanism of immune evasion leading to recurrence or chronicity of infections, and further bacterial dissemination.[9,16]

Dermal fibroblasts are cellular key players in physiologic wound healing[3] since they proliferate and produce extracellular matrix proteins to fill up the wound.[1] Although the diverse effects of SA on the immune system have been described, its effect on fibroblast functions in the context of dermal wound healing, and especially its contribution to non-healing DUs in SSc, has not yet been investigated. Therefore, we evaluated the interaction of SA and dermal fibroblasts with respect to key tissue repair functions including potential signaling pathways.

2 | MATERIALS AND METHODS

2.1 | Study subjects

Human primary dermal fibroblasts were obtained from lesional skin of patients with diffuse cutaneous (dc) SSc (n = 3) and

from skin biopsies from healthy controls (HC) (n = 3) as previously described.[17] Wound swabs of DU were subjected to routine microbiology diagnostics in 30 SSc patients. The main characteristics of the analyzed SSc patients (n = 30) at the time of the microbial sampling are provided in Table 1. Written informed consent was obtained. The study was approved by the Zurich ethics committee (pre-BASEC-EK-839, BASEC KEK-no. 016-01515, BASEC-no. 2014-0197, KEK-no. 2018-0187). Patients/public were not involved in the study.

2.2 | Cell culture

Human primary dermal fibroblasts were obtained from forearms of dcSSc patients and HCs at the department of Rheumatology, University Hospital Zurich. Skin was minced into small pieces with a sterile scalpel. The pieces were transferred to a 6-well plate with the dermis facing the bottom of the plate. The skin pieces were incubated with complete cell culture medium (DMEM containing 10% fetal calf serum (FCS), 50 units/mL of penicillin, 50 μg/mL of streptomycin and 100 μM of 2-mercaptoethanol) to let fibroblasts outgrow from the skin for at least two weeks. Cells were passed 3 times to get rid of other cell types and expand the culture. The purity of the obtained fibroblasts was confirmed by FACS analysis and immunofluorescence. FACS analysis revealed that more than 90% of cells were CD90+CD45-CD31-. Immunofluorescence showed robust expression of alpha-smooth muscle actin and stress fiber upon TGF-beta stimulation (Figure S1). These results suggested that our primary fibroblasts consisted of a sufficiently pure cell population.

Primary dermal fibroblasts were cultured in the complete cell culture medium. Human neonatal fibroblasts immortalized with hTERT (BJ-5ta, ATCC CRL-4001) were cultured in DMEM and Medium 199 (mix ratio 4:1; Sigma-Aldrich, St Louis, MO) containing 10% FCS and 0.01 mg/mL of hygromycin (Sigma-Aldrich) at 37°C in 5% carbon dioxide. Cells were stimulated with 1×10^5 or 1×10^7 CFU/mL of live SA (ATCC 6538; kindly provided by A. S. Zinkernagel) or 1×10^8/mL of HKSA (InvivoGen, San Diego, CA), and then were used for each subsequent analysis. The maximum bacterial load was determined by cytotoxicity assay using Cell Counting Kit-8 (CCK-8; Dojindo Molecular Technologies, Rockville, MD). Treatment of both primary human dermal fibroblasts and BJ-5ta cells with SA at a bacterial load within a range of 1×10^4-5×10^7 was found to have no cytotoxic effect (>95% viability) on such cells.

2.3 | Bacterial strain and bacterial co-culture stimulation system

SA (ATCC 6538) was stored in Tryptic soy broth (TSB; BD Biosciences, San Jose, CA) medium containing 20% glycerol at −20°C. Bacteria were cultured in 3 mL of TSB medium in a

TABLE 1 Patients' main characteristics

Parameters	Numbers
Age (years)	42 (20-79)
Gender (m/f)	3/27 (10/90%)
Disease duration (years)	8 (0-49)
Skin involvement	
Limited cutaneous	12 (40%)
Diffuse cutaneous	15 (50%)
Only sclerodactyly	3 (10%)
Raynaud's phenomenon	30 (100%)
Presence of active digital ulcers	30 (100%)
Number of digital ulcers	3 (1-20)
Auto-antibody status	
ANA	28 (93%)
Anti-Centromere	18 (60%)
Anti Scl-70	14 (47%)
Anti RNA-Polymerase	6 (20%)
Anti-U1nRNP	3 (10%)
Organ involvement	
Pulmonary arterial hypertension	4 (13%)
Lung fibrosis (HRCT scan)	16 (53%)
Esophageal symptoms	23 (77%)
Intestinal symptoms	17 (57%)
Stomach symptoms	17 (57%)
Renal crisis	0 (0%)
Immunosuppressive therapy	10 (30%)

Note: Data are presented as absolute numbers (percentages) or medians (ranges).

10 mL Falcon round bottom tube for 18 h at 37°C in an incubator shaker to reach the early stationary phase for use in the co-culture system. The bacterial concentration was estimated by measuring the optic density of bacterial suspension with an optical densitometer (BioRad, Hercules, CA). Bacteria were harvested by centrifugation at 4200 *g* for 10 min. The bacterial pellet was washed with phosphate-buffered saline (PBS) twice and then suspended in DMEM supplemented with 1% human albumin (Sigma-Aldrich) and 25 mM of HEPES (Thermo Fisher Scientific, Waltham, MA) (invasion medium). The bacteria containing medium was then added to a monolayer of cultured fibroblasts,[16,18] plated as per assay requirements. Stimulation of fibroblasts was unopposed by antibiotics for 3 h. Thereafter DMEM with 1% FCS supplemented with the antibiotic flucloxacillin sodium (0.1 mg/mL) (Sigma-Aldrich) was added. The concentration was determined by bacteria killing assay to minimize undesirable effects on fibroblasts.

2.4 | ELISA

One hundred thousand cells were cultured in a 6-well plate. After 24 h starvation with 1% FCS, cells were washed with PBS and treated with the indicated amount of SA as described above. After 72 h incubation, the supernatants were collected. The levels of IL-1β, IL-6, IL-8, IFN-β and procollagen Iα1 in the co-culture supernatants were quantified using ELISA assays (R&D Systems, Minneapolis, MN) and a microplate reader (Biotek Instruments, Winooski, VT) according to the manufacturer's protocols.

2.5 | Quantitative real-time PCR (qPCR) analysis

Fifty thousand cells were cultured in a 12-well plate. After a 24 h starvation with 1% FCS, cells were washed with PBS and treated with the indicated amount of SA as described above. After 24 h incubation, cells were washed with PBS and total RNA samples were prepared using a Quick-RNA MicroPrep Kit (Zymo research, Irvine, CA). Synthesis of cDNA was performed using a Transcriptor First Strand cDNA Synthesis Kit (Roche, Basel, Switzerland). Quantitative PCR was performed using a Stratagene Mx3005P Quantative PCR System (Agilent Technologies, Santa Clara, CA) making use of a SYBR green reagent (Promega, Madison, WI). The levels of each gene were normalized to the levels of RPLP0. The sequences of primers used are presented in Table 2.

2.6 | Migration assay

Migration assays were performed as described[19] using a 2-well cell culture insert (Ibidi, Planegg, Germany) allowing for an equal gap down the center of a cellular monolayer. After bacterial co-culture, serial imaging of fibroblast migration was performed using an imaging system (IX81; Olympus, Tokyo, Japan) equipped with excellencePro software (Olympus). Fibroblast migration was measured by assessing the percentage of the gap still uncovered by fibroblasts at various time intervals using ImageJ software (NIH, Bethesda, MD).

2.7 | Cell contraction assay

A collagen solution (400 μL) was prepared from the cell contraction assay kit (Cell Biolabs, San Diego, CA) and mixed with 100 μL of cell-bacteria solution. The solution was plated in a 24-well culture plate and incubated for 1 h to allow polymerization of the collagen gel. Thereafter, 1000 μL of the DMEM (Sigma-Aldrich) containing 1% FCS was added to each well, followed by flucloxacillin after 2 h. After 48 h, the gel was gently released from the sides of the well and after further 6 h, the area of each gel was measured using ImageJ software.

Gene symbol	Primer sequence
RPLP0	Forward primer: 5′-ACA CTG GTC TCG GAC CTG AGA A-3′
	Reverse primer: 5′-AGC TGC ACA TCA CTC AGA ATT TCA-3′
MMP1	Forward primer: 5′-CTC TGG AGT AAT GTC ACA CCT CT-3′
	Reverse primer: 5′-TGT TGG TCC ACC TTT CAT CTT C-3′
MMP3	Forward primer: 5′-TCA CTC ACA GAC CTG ACT CG-3′
	Reverse primer: 5′-AAA GCA GGA TCA CAG TTG GC-3′
TLR2	Forward primer: 5′-CTG TGC TCT GTT CCT GCT GA-3′
	Reverse primer: 5′-GAT GTT CCT GCT GGG AGC TT-3′
TLR9	Forward primer: 5′-AAT CCC TCA TAT CCC TGT CCC-3′
	Reverse primer: 5′-GTT GCC GTC CAT GAA TAG GAA G-3′
MYD88	Forward primer: 5′-GCA CAT GGG CAC ATA CAG AC-3′
	Reverse primer: 5′-GAC ATG GTT AGG CTC CCT CA-3′
ZBP1	Forward primer: 5′-AAC ATG CAG CTA CAA TTC CAG A-3′
	Reverse primer: 5′-AGT CTC GGT TCA CAT CTT TTG C-3′
CGAS	Forward primer: 5′-ACA TGG CGG CTA TCC TTC TCT-3′
	Reverse primer: 5′-GGG TTC TGG GTA CAT ACG TGA AA-3′
IFI16	Forward primer: 5′-TAG AAG TGC CAG CGT AAC TCC-3′
	Reverse primer: 5′-TGA TTG TGG TCA GTC GTC CAT-3′
TMEM173	Forward primer: 5′-CAC TTG GAT GCT TGC CCT C-3′
	Reverse primer: 5′-GCC ACG TTG AAA TTC CCT TTT T-3′
IL1B	Forward primer: 5′-ATG CAC CTG TAC GAT CAC TG-3′
	Reverse primer: 5′-ACA AAG GAC ATG GAG AAC ACC-3′
IL6	Forward primer: 5′-CTC TTC AGA ACG AAT TGA CAA ACA A-3′
	Reverse primer: 5′-GAG ATG CCG TCG AGG ATG TAC-3′
IL8	Forward primer: 5′-TTG GCA GCC TTC CTG ATT TC-3′
	Reverse primer: 5′-TGG CAA AAC TGC ACC TTC AC-3′
IFNB1	Forward primer: 5′-GTC ACT GTG CCT GGA CCA TAG-3′
	Reverse primer: 5′-GTT TCG GAG GTA ACC TGT AAG TC-3′

2.8 | Proliferation assay

Cells were seeded into a 96-well plate. After 24 h starvation, the cells were cultured with SA as described above. After 72 h, cell proliferation was assessed by CCK-8 according to the manufacturer's protocol. The absorbance was then read at 450 nm using a microplate reader (Biotek Instruments).

2.9 | Apoptosis and necrosis assay

Cells were seeded into a white 96-well plate. After overnight culture, the cells were cultured with SA as described above. After 3 h of bacterial co-culture, apoptosis and necrosis were assessed at 7 h (4 h after flucloxacillin was added) using RealTime-Glo Annexin V Apoptosis and Necrosis Assay (Promega). Chemiluminescence and fluorescence were measured using a microplate reader.

2.10 | Invasion assay

One hundred thousand cells were cultured in a 6-well plate. After 24 h starvation, cells were washed twice with PBS and treated with the indicated amount of SA in invasion medium for 3 h. Hereafter, the supernatant was aspirated and the cells were treated with lysostaphin (Sigma-Aldrich), which is an antibacterial endopeptidase, for 1 h to eradicate extracellular bacteria. Cells were washed once with PBS and then lysed with distilled water. The lysate containing intracellular bacteria was diluted and seeded on agar plates. Bacterial invasion was quantified by counting the number of bacterial colonies on the plates.[20]

2.11 | Immunofluorescence and confocal microscopy

Glass cover slips with a diameter of 12 mm were placed in 24-well plates. Thereafter, 5×10^4 fibroblasts (in

500 μL/well) in DMEM with 1% FCS (1% FCS-DMEM) were added and starved for 24 h. SA cultures were grown overnight in 5 mL TSB and then adjusted to reach 2×10^8 CFU/mL. Cells were infected with MOI (multiplicity of infection) 1 (1×10^5 CFU/mL) or 100 (1×10^7 CFU/mL) in 1% FCS-DMEM. After 3 h of bacterial invasion, the supernatants were aspirated and cells were fixed with 4% paraformaldehyde. Nucleic acids (eukaryotic nuclei and bacteria) were then stained with 20 μM Hoechst reagent, washed once with PBS, and then blocked with PBS supplemented with 1% bovine serum albumin (1% BSA-PBS). Thereafter, 1:100 rhodamine phalloidin (Invitrogen, Waltham, MA) was added to stain actin. After the removal of the blocking buffer and the actin dye, a mouse monoclonal primary antibody against SA (clone 704; Abcam, Cambridge, MA) was added in 1% BSA-PBS at a final concentration of 2 μg/mL. After washing once with PBS, a goat anti-mouse antibody Alexa 488 (Invitrogen) was added in 1% BSA-PBS at a final concentration of 4 μg/mL. To stain late endosomes, a mouse primary antibody against LAMP2 (BD Biosciences) and a goat anti-mouse antibody Alexa 488 (Invitrogen) were used. For identification of intracellular SA in Figure 3, CFSE (carboxyfluorescein succinimidyl ester)-labeled SA or HKSA were used. After washing once with PBS, cells were mounted in ProLong Gold (Invitrogen) on glass slides. Images were obtained with an inverted SP8 confocal laser scanning microscope (Leica, Wetzlar, Germany).

2.12 | Blockade of endocytosis

Cells were treated with 10 μg/mL of cytochalasin D (Sigma-Aldrich) for 1 h. After the cells were washed with PBS, bacteria containing medium were added to the wells to examine the effect of bacterial invasion on cell death or expression of IFN-β and inflammatory mediators.

2.13 | Gene knockdown by siRNA

Human MYD88 siRNA, human TMEM173 siRNA, and AllStars Negative Control siRNA were purchased from Qiagen (Venlo, Netherlands). The sequences of the siRNAs are shown in Table 3 below.

Fifty thousand cells were cultured without antibiotics in a 12-well plate. After overnight culture, siRNA-Lipofectamine2000 (Thermo Fisher Scientific) complexes in Opti-MEM I Reduced Serum Medium (Thermo Fisher Scientific) were prepared for each transfection sample. The siRNA-Lipofectamine complexes were added to each well, and the cells were incubated in a humidified CO_2 incubator. The final concentration of each siRNA was 20 nM. After 6 h incubation, the cell culture medium was changed to fresh DMEM with 1% FCS. After further 18 h incubation, the cells were used for each gene knockdown assay.

2.14 | Statistical analysis

Data are summarized as medians or means depending on the experimental setting. The statistical analysis was performed using Prism 8.1 (GraphPad Software, San Diego, CA). The respective statistical analyses are specified in each figure legend. P values <.05 were considered significant.

2.15 | FACS analysis

Cells were co-cultured with the indicated amount of SA for 24, 48, or 72 h. Cells were treated with 2 μM of monensin (Sigma-Aldrich) for the final 6 h. Cells were washed and incubated with LIVE/DEAD Fixable Near-IR Dead Cell Stain (Thermo Fisher Scientific) for 30 min. Thereafter, anti-CD45-eFluor 450 (clone HI30), anti-CD31-Super Bright 600 (clone WM-59) (Thermo-Fischer Scientific), and anti-CD90-APC (clone 5E10; BD Biosciences) antibody for 30 min at 4°C. Cells were then fixed with Cytofix/Cytoperm Cell Permeabilization/Fixation Solution (BD) for 15 min at 4°C. Cells were then washed and incubated with anti-IL-6-PE (clone MQ2-6A3, BD), anti-IL-8-PE (Clone 8CH, Thermo Fisher) or anti-IFN-β-Fluorescein (Clone MMHB-3, R&D Systems) for 30 min at 4°C. Purity of primary fibroblasts and level of intracellular cytokine expression were analyzed on a flow cytometer (Attune NxT, Thermo Fisher). Flow cytometry data were analyzed with FlowJo (v10.2, BD).

TABLE 3 siRNA sequences for TME173 and MYD88

siRNA	Sequence
TMEM173	Target Sequence: 5′-CCG CAC GGA TTT CTC TTG AGA-3′
	Sense strand: 5′-GCA CGG AUU UCU CUU GAG AUU-3′
	Antisense strand: 5′-UCU CAA GAG AAA UCC GUG CGG-3′
MYD88	Target Sequence: 5′-CAG GAC CAG CTG AGA CTA AGA-3′
	Sense strand: 5′-GGA CCA GCU GAG ACU AAG AUU-3′
	Antisense strand: 5′-UCU UAG UCU CAG CUG GUC CUG-3′

2.16 | Immunofluorescence of human primary dermal fibroblasts

Cells were cultured on an 8-well chamber slide (Thermo Scientific) with 10 ng/mL of TGF-β1 for 72 h. Cells were then washed and fixed with 4% paraformaldehyde for 5 min. Cells were permeabilized with 0.1% Triton X-100 (Sigma-Aldrich) for 5 min. After blocking with 10% FCS for 20 min, cells were incubated with anti-actin, α-smooth muscle (clone 1A4; Sigma-Aldrich) for 1 h at room temperature. Cells were then washed and incubated with anti-mouse IgG-Alexa Flour 488 (Thermo Fischer Scientific) and phalloidin-TRITC (Sigma-Aldrich) for 45 min. Nucleic acids were then stained with DAPI (4′,6-diamidino-2-phenylindole; Roche). After washing with PBS, cells were mounted in fluorescence mounting medium (Dako) and images were obtained with a fluorescence microscope (DP80, Olympus).

2.17 | Cell count

Fifty thousand cells were co-cultured with the indicated amount of SA for 24, 48, or 72 h on 12-well plates. Cells were stained with trypan blue. Live and dead cells were then determined using an automated cell counter (TC10, Bio-Rad).

3 | RESULTS

3.1 | Chronic DU of SSc patients are colonized by SA

To assess which bacteria are predominantly found in chronic DU, we analyzed wound swabs of 30 SSc patients from our department. Most patients with DU showed positive results with mostly moderate (CFU = 10^4-10^5/mL, ie, critically colonized; 30%) or plentiful bacterial growth (CFU >10^5-10^6/mL, ie, infected; 37%), while only 5 (17%) did not show any growth at all. In 53% of dermal wounds, SA was detected. Other detected bacterial strains included *Pseudomonas aeruginosa*, *Haemophilus parainfluenzae*, *Enterobacter cloacae*, *Enterococcus faecalis*, *Streptococcus pyogenes*, *Klebsiella pneumoniae*, *Proteus vulgaris*, *Staphylococcus lugdunensis*, and *Staphylococcus epidermidis*. In SA-positive wounds, deep soft tissue infections (n = 7, 43.8%) and osteomyelitis (n = 5, 31.3%) occurred more often. These findings are in accordance with previous reports.[10,11]
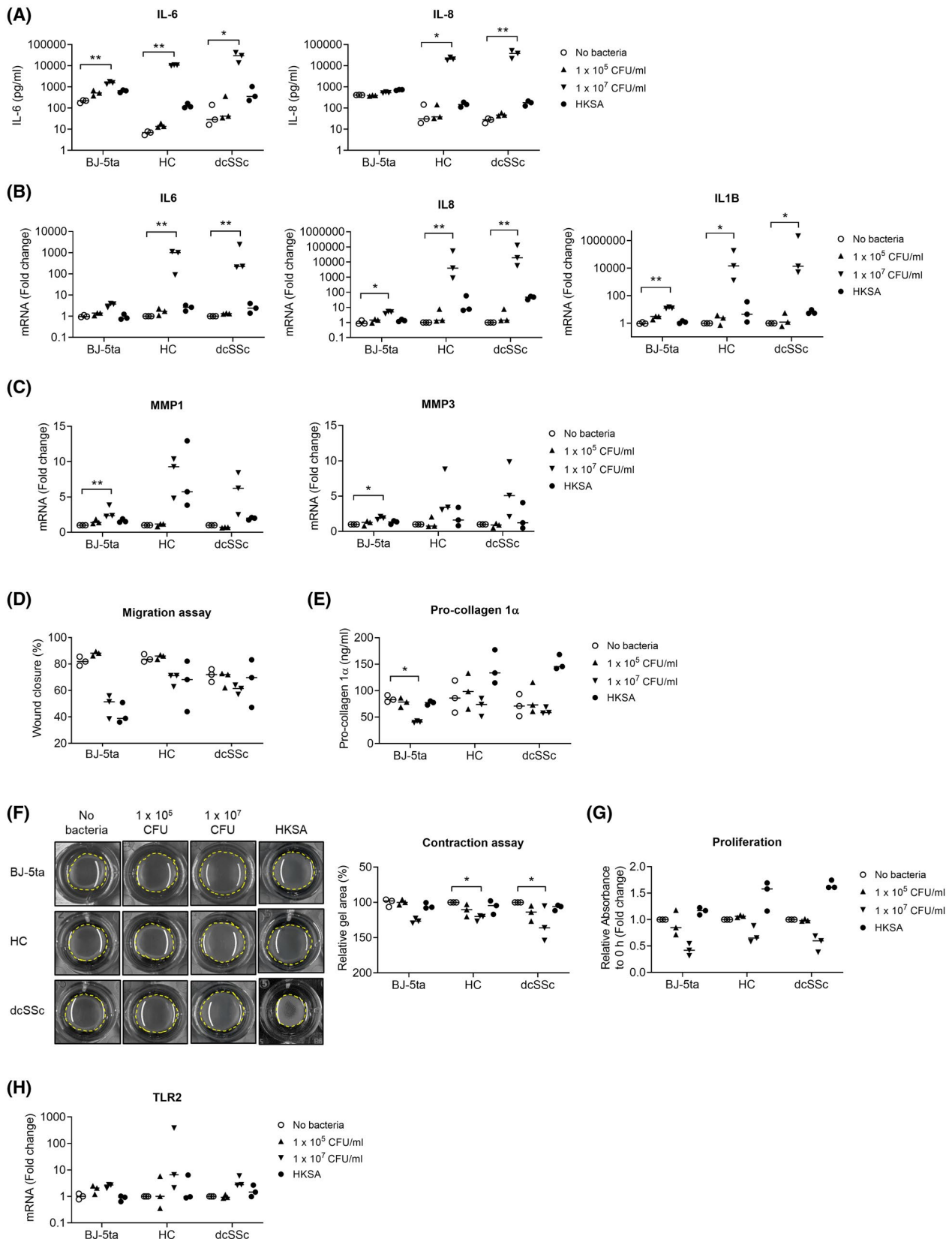
3.2 | SA affects key functions of dermal fibroblasts

To investigate the impact of SA-fibroblast interactions on tissue repair we first co-cultured dermal fibroblasts (BJ-5ta)

with live SA. We deliberately chose a cell line for the first evaluation step in order to avoid the potential heterogeneity of results that might arise from the use of primary cells. A lower inoculum representing colonization (1×10^5 CFU/mL) and a higher inoculum reflecting infection (1×10^7 CFU/mL) were used.[21] We confirmed dose-dependent effects of SA between 1×10^5 and 1×10^7 CFU/mL on some fibroblast functions (Figure S2).

Exposure to the higher inoculum influenced several important fibroblast functions. The secretion of IL-6 and IL-8 by dermal fibroblasts was increased to 1340 pg/mL ($P < .05$) and to 120 pg/mL ($P = .12$), respectively (Figure 1A). IL-1β was not detected by ELISA (data not shown) at 72 h. The gene expression was likewise upregulated for IL-6/-8 (Figure 1B). Although the gene expression of IL-1β was also upregulated (Figure 1B), the expression level relative to ribosomal protein lateral stalk subunit P0 (RPLP0) was much lower than those of IL6 and IL8 (data not shown) consisting with no detection of IL-1β protein. The increased secretion and gene expression of the cytokines were already observed at 24 h (Figure S3). In addition, we observed an upregulated gene expression of MMP1 by 2.8-fold ($P < .05$) and MMP3 by 1.9-fold ($P < .05$) (Figure 1C). Wound closure as assessed by migration was reduced by 34% at 16 h ($P = .64$) (Figure 1D). Type 1 collagen synthesis was significantly decreased in 1×10^7 CFU/mL of SA-challenged BJ-5ta cells (Figure 1E). Collagen gel contraction as measure of fibroblast contractility was impaired by 26% ($P = .05$) (Figure 1F). Proliferation was reduced by 57% ($P = .26$) (Figure 1G). Live cell numbers and proportions of live cells at 24 h and 72 h were also assessed. Live cells were decreased to around 50% compared with controls without SA-exposure at 72 h (Figure S4). Given that the cell number was reduced by exposure to higher dosages of SA, we performed intracellular cytokine staining to assess the production of cytokines while controlling for the cell number. The FACS analyses revealed that the higher dosages of SA increased the production of the cytokines by human dermal fibroblast at the single cell level (Figure S5).

To confirm the effects observed in BJ5-ta cells, we next assessed tissue repair mechanisms in primary cells. Fibroblasts from HC and dcSSc patients were co-cultured with live SA. As previously observed for the BJ-5ta cells, only exposure to the higher inoculum influenced several important fibroblast functions. The secretion of IL-6 and IL-8 by dermal fibroblasts was increased to 10 730/30 000 pg/mL (HC/dcSSc; $P < .05$ each) and to 20 340/38 170 pg/mL (HC/dcSSc; $P < .05$ each), respectively (Figure 1A). IL-1β was not detected by ELISA (data not shown). The gene expression was likewise upregulated for IL-6/-8/-1β (Figure 1B). Compared with the BJ-5ta cell line, these effects were more pronounced. This was also true for the upregulation of MMP1 and MMP3 mRNA (Figure 1C). The gene expression of MMP1 was increased by 9.3/6.2-fold (HC/dcSSc; $P = .07$/= .12) and MMP3 by 3.4/5.1-fold

FIGURE 1 *S aureus* (SA) affects key functions of dermal fibroblasts. A, The concentration of IL-6 and IL-8 in the culture supernatants was quantified at 72 h by ELISA. B, The gene expression of IL-6, IL-8, and IL-1B was assessed at 72 h by qPCR analysis. C, MMP1 and MMP3 mRNA levels were evaluated at 24 h by qPCR analysis. D, Migration assay was performed at 16 h (BJ-5ta cells) or 28 h (primary cells). E, Pro-collagen 1α concentration in the culture supernatants was quantified at 72 h by ELISA. F, Cell contractility was evaluated at 48 h by collagen gel contraction assay. G, Cell proliferation was evaluated at 72 h using CCK-8. H, TLR2 mRNA levels were measured by qPCR at 24 h. Bars show medians, n = 3 per group. *$P < .05$, **$P < .01$ (Kruskal-Wallis test followed by Dunn's multiple comparisons test)

(HC/dcSSc; $P = .16$ each) (Figure 1C). Wound closure as assessed by migration was reduced by 12/11% at 28 h (HC/dcSSc; $P = .23/= .24$) (Figure 1D). There was a trend toward a decreased secretion of pro-collagen Iα (Figure 1E). Collagen gel contraction as a measure of fibroblast contractility was impaired by 20/36% (HC/dcSSc; $P < .05$ each) (Figure 1F). Proliferation was reduced by 0.65/0.60-fold (HC/dcSSc; $P = .91/= .26$) (Figure 1G). The observed effects for cell migration, contraction, and cell proliferation were similar compared to these in BJ-5ta cells. Overall, these results suggest that various fibroblast effector functions are affected by SA, with potential implications for wound healing.

3.3 | Effects of heat-killed SA on fibroblast functions are less pronounced as compared to live SA

Cell wall components of SA can exert pro-inflammatory effects via Toll-like receptor (TLR) 2-mediated innate immune responses.[22] Therefore, we assessed whether not only live SA, but also heat-killed SA (HKSA) affected mechanisms of tissue repair in dermal fibroblasts. TLR2 was constitutively expressed in dermal fibroblasts. Expression was not further upregulated upon SA exposure (Figure 1H). The secretion and the mRNA upregulation of IL-6, IL-8, IL-1β (Figure 1A,B) and the upregulation of MMP1/3 mRNA (Figure 1C) upon HKSA stimulation were much lower than upon live SA exposure. HKSA had no significant negative effects on migration, type 1 collagen synthesis, contractility, or proliferation (Figure 1D-G). These results suggest that only live SA has an effect on the assessed tissue repair mechanisms. Again, no differences were observed for fibroblasts from different sources.

3.4 | SA induces cell death in dermal fibroblasts and invades dermal fibroblasts by endocytosis

As live SA has been shown to induce cell death in other cell types,[15] we examined whether this also applied to dermal fibroblasts. Using a real time assay, we found that SA increased both apoptosis by 10.9-fold (BJ-5ta; $P < .05$) (Figure 2A) and necrosis by 4.2-fold (BJ-5ta; $P < .05$) (Figure 2B). This was again confirmed in primary cells, where apoptosis was increased by 5.2/5.4-fold (HC/dcSSc; $P < .05/.14$) (Figure 2A) and necrosis by 9.5/10.2-fold (HC/dcSSc; $P < .05$ each) (Figure 2B). The occurrence of cell death was time-dependent. High dosages of SA induced apoptosis and necrosis at earlier time points than at 24 h and 72 h (Figure S6A,B).

Based on recent studies suggesting intracellular uptake and prolonged persistence of SA in non-professional phagocytes,[9,16,23,24] we next investigated whether this applied to human dermal fibroblasts by assessing the colony-forming unit (CFU) recovery rate.[20] We confirmed that lysostaphin, which was used to eradicate extracellular bacteria, sufficiently worked by confocal microscopic analysis (Figure 3B). Already at the lower inoculum representing colonizing conditions, but to a much larger extent at the higher inoculum mimicking infection, up to 60% of inoculated SA invaded primary dermal fibroblasts. Both HC and dcSSc fibroblasts showed a trend toward a higher intracellular uptake of SA as compared to BJ-5ta cells (Figure 2C). This is in line with the observed higher levels of IL-6/IL-8 secretion and the mRNA upregulation of IL6, IL8, IL1B, MMP1, and MMP3 in both HC and dcSSc fibroblasts upon co-culture with live SA (Figure 1). The invasion of dermal fibroblasts was further confirmed by confocal microscopy. Intracellular SA was detected in the BJ-5ta cell line and both primary HC and SSc fibroblasts (Figure 2D). In contrast, HKSA was rarely detected in BJ-5ta cells (Figure 3B). The images of HC and dcSSc fibroblasts are shown in Figures S7 and S8, respectively.

In non-professional phagocytes, adhesin-mediated endocytosis has been suggested as a potential mechanism for the intracellular uptake.[25-27] Intra-endosomal bacteria can be detected by co-staining with Lamp-2.[28] Using confocal microscopy, we detected CFSE-labeled SA co-stained with the endosomes of dermal fibroblasts (Figure 3A). We next examined whether SA invasion affected cell death using an endocytosis inhibitor, cytochalasin D. Cytochalasin D inhibited the internalization of bacteria (Figure 3B). The inhibition of endocytosis increased the rate of cell death in dermal fibroblasts (Figure 3C,D) suggesting that extracellular cytolytic toxins of SA rather than host cell death due to internalization and phagosomal escape drive cell death in infected dermal fibroblasts.[13,15]

3.5 | Intracellular SA activates both host defense and immune evasion responses via dsDNA sensors involving MyD88 and STING signaling pathways

Next, we evaluated whether the presence of intracellular SA could activate pathways explaining the observed effects on dermal fibroblasts upon co-culture with SA. In non-professional phagocytes, intracellular bacteria are either inactivated by lysosomal proteases or by autophagy with subsequent release of bacterial DNA into the cytosol, where it is recognized by cytosolic pattern recognition receptors.[9,29,30] These include TLR8/9,[31,32] nucleotide oligomerization domain (NOD) 2,[33] the NOD-like receptor 3 (NLRP3),[34] and absent in melanoma 2 (AIM2),[35] some of
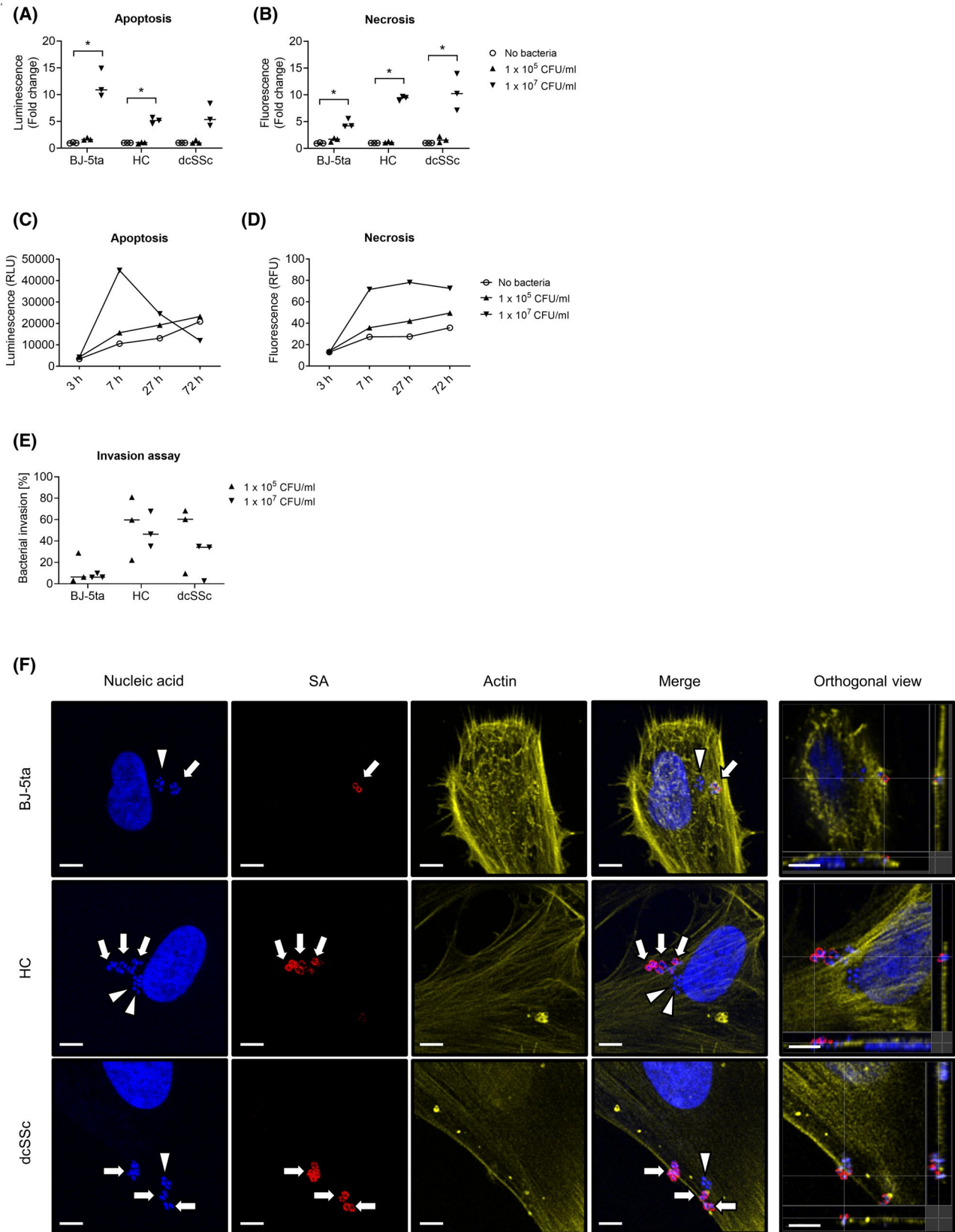
FIGURE 2 SA induces cell death in dermal fibroblasts and invades dermal fibroblasts. Apoptosis (A) and necrosis (B) were assessed at 7 h. Bars show medians, n = 3 per group. *P < .05 (Kruskal-Wallis test followed by Dunn's multiple comparisons test). C, SA invasion of dermal fibroblasts. Bars show medians, n = 3 per group. The Kruskal-Wallis test followed by Dunn's multiple comparisons test was performed within each SA load. D, Representative pictures of intracellular (arrow heads; blue) and extracellular (arrows; magenta) SA are shown. Scale bar = 5 μm
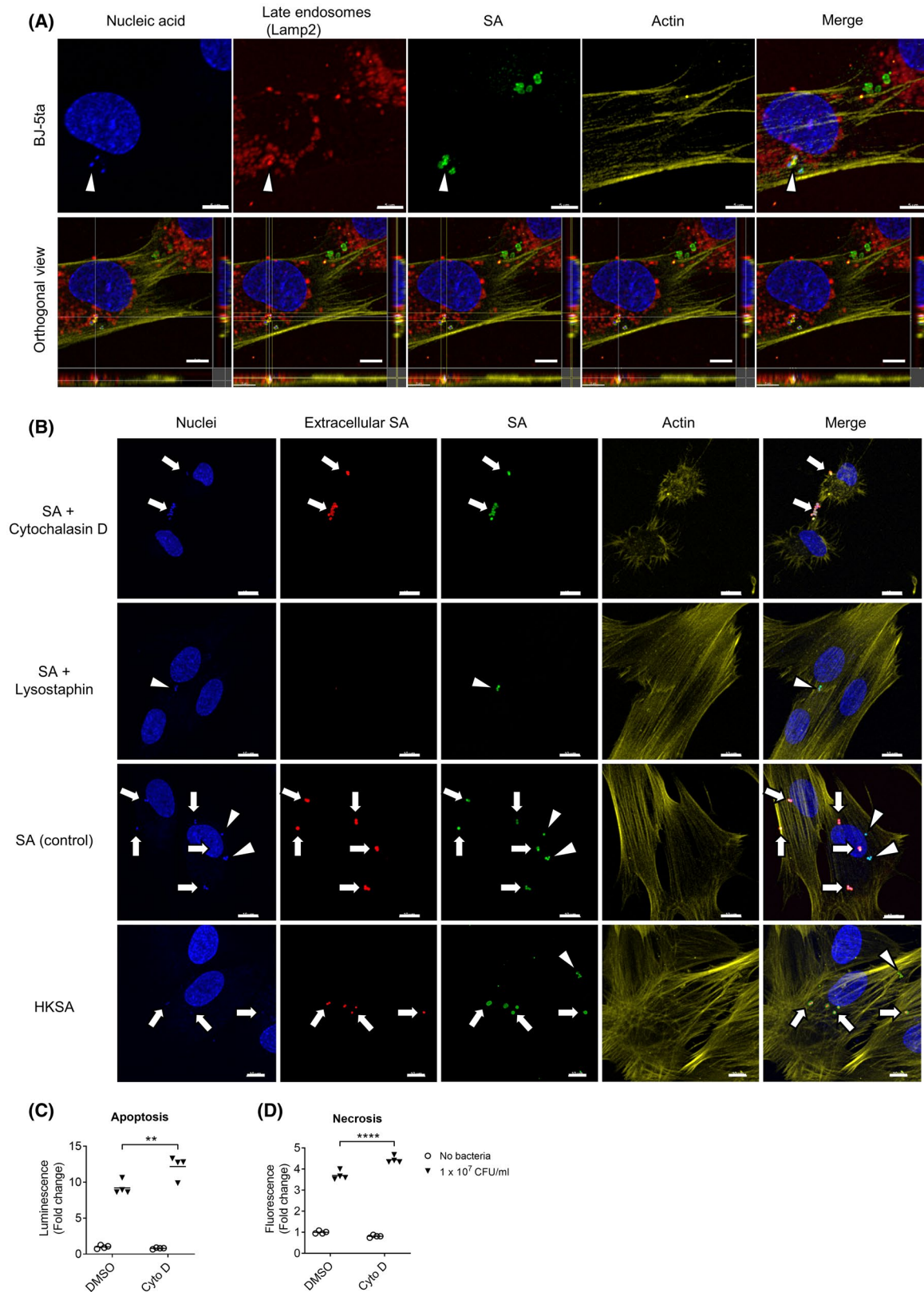
FIGURE 3 SA invades dermal fibroblasts by endocytosis, but the invasion does not promote cell death. A, Representative pictures of intra-endosomal SA (arrow heads) in BJ-5ta cells are shown. SA was labeled with CFSE. Scale bar = 5 µm. B, Effect of cytochalasin D on SA internalization, effect of lysostaphin treatment on removal of SA, and internalization of HKSA were assessed respectively in BJ-5ta cells. Intracellular (arrow heads) and extracellular (arrows) are shown. SA and HKSA were labeled with CFSE. Scale bar = 10 µm. C and D, BJ-5ta cells were treated with an endocytosis inhibitor, cytochalasin D (10 µg/mL) for 1 h before SA exposure. Apoptosis (C) and necrosis (D) were evaluated at 7 h. Bars show means, n = 4 per group. $**P < .01$, $****P < .0001$ (Two-way ANOVA followed by Sidak's multiple comparisons test)

which converge on the adaptor protein, myeloid differentiation factor 88 (MyD88), which plays an important role in the host defense against SA with induction of IL-1β, IL-6, and IL-8. On the other hand, SA can also induce a type I IFN response, which has been associated with immune evasion and involves MyD88 signaling via its downstream targets IRF5 and IRF7 (interferon regulatory factors).[36] Recent data on SA-mediated intracellular signaling in monocytes identified the adaptor protein, stimulator of interferon genes (STING), as a central part of the type I IFN response via activation of TANK-binding kinase 1 (TBK1) and IRF3.[37] However, the STING-TBK1 axis can also induce NF-κB signaling with production of inflammatory cytokines including IL-6 and TNF-α.[38]

Because we found bacterial DNA in the endosomes of dermal fibroblasts as well as in the cytoplasm (Figures 2D and 3A), we hypothesized that MyD88 and STING might be centrally involved in the regulation of fibroblast functions by SA via intracellular DNA sensor molecules. The TLR9 gene, an endosomal/lysosomal DNA sensor, was constitutively expressed in dermal fibroblasts, yet not substantially upregulated upon SA exposure (Figure 4A). In contrast, its downstream target, MyD88 became significantly upregulated on mRNA level (Figure 4A). The same applied to the gene of STING, TMEM173, and its upstream cytosolic dsDNA sensor molecules DAI/ZBP1 (DNA-dependent activator of IFN-regulatory factors/ Z-DNA binding protein 1), cGAS (cyclic GMP-AMP synthase), and IFI16 (IFN gamma-inducible protein 16) in infectious conditions (Figure 4B).

As downstream target of both MyD88 and STING, and as a key factor of SA for evasion of host defense, we analyzed the induction of IFN-β upon SA exposure on mRNA and protein level (Figure 4C). Indeed, live SA increased IFN-β secretion in dermal fibroblasts under infectious conditions up to 24/34/35 pg/mL (BJ-5ta/HC/dcSSc; $P < .05$ each). Of note, in contrast to live SA, HKSA had neither a relevant effect on the expression of intracellular DNA sensor genes (Figure 4D) nor on the secretion of IFN-β (Figure 4E).

To confirm the importance of STING and MyD88 for the induction of both the immune evasion response (type I IFN) and the host defense response (IL-6, IL-8, IL-1β), we performed knockdown experiments with small interfering RNA (siRNA). TMEM173 siRNA and MYD88 siRNA decreased the expression of their respective target genes (Figure 5A). Knockdown of STING or MyD88 reduced the induction of IFN-β (down to 68/66%; $P = .07/.06$), IL-6 (down to 57/55%; $P < .01/<.001$), IL-8 (down to 45/36%; $P < .001$, each), and IL-1β (down to 79/66%; $P < .01/<.001$) (Figure 5B).

Endocytosis blockade with cytochalasin D hindering entry of SA into the cells largely decreased the expression of IFN-β (down to 26%; $P < .0001$), IL-6 (down to 32%; $P < .05$) and IL-8 (down to 28%; $P < .05$), but not IL-1β (Figure 5C).

Taken together, these results suggest that the activation of STING and MyD88 pathways is crucial for the induction of IFN-β, IL-6, IL-8, and IL-1β, following the invasion of fibroblasts by live SA (Figure 6).

4 | DISCUSSION

Our study showed that infection of dermal fibroblasts with live SA induces inflammation and tissue destruction by impairing fibroblast functions. Results from the BJ-5ta fibroblast cell line were confirmed with primary cells from healthy individuals and dcSSc patients. No significant differences regarding the net effects on tissue repair functions between these dermal fibroblasts from different sources were observed in vitro.

Chronicity, recurrence, and antibiotic resistance of (wound) infections is a major concern worldwide.[1,39,40] Herein, we provide novel evidence for SA-induced immune evasion responses by dermal fibroblasts with profound potential impact for non-healing wounds. Infection is a contributing factor in both the development and persistence of chronic wounds. Bacterial colonization occurs in all wounds although the microbial burden varies.[1,7] Acute immune responses upon tissue injury could prevent the development of bacterial infection.[7] However, prolonged inflammation may impair tissue repair processes.[3] The skin acts as a physical barrier against invading pathogens. If the basement membrane is breached, dermal tissue and cells are exposed to commensal skin bacteria.[9] Fibroblasts are not only important for sustaining the tissue and organ architecture. As shown in our study, they also produce chemokines such asIL-8 and MCP-1 as well as IL-6 to recruit neutrophils, macrophages, and lymphocytes thereby supporting these immune cells to reduce the bacterial burden.[41] Thus, fibroblasts initiate inflammation as sentinel cells upon tissue injury and/or local infection.[41,42] We showed that in the SA co-culture setting, human primary dermal fibroblasts also acted as non-professional phagocytes resulting in the intracellular uptake of up to 60% of bacteria, which was at least partially mediated by endocytosis as demonstrated by the blocking experiments with cytochalasin D. In non-professional phagocytes, the interaction of fibronectin (Fn), SA Fn-binding proteins, and integrins was shown to be a key element of SA-induced endocytosis.[27]

The opportunistic pathogen, SA escapes not only the host immune defense, but also anti-infective therapy in non-professional phagocytes.[23] The post-invasion effects vary depending on the cell type, but prolonged "hibernation" periods have been shown in osteoblasts, epithelial/endothelial cells and murine fibroblasts.[15] Interestingly, another immune evasion reaction, that is the induction of a type I IFN response, was mainly mediated by intracellular SA. Herein, we provided some evidence that a variety of intracellular
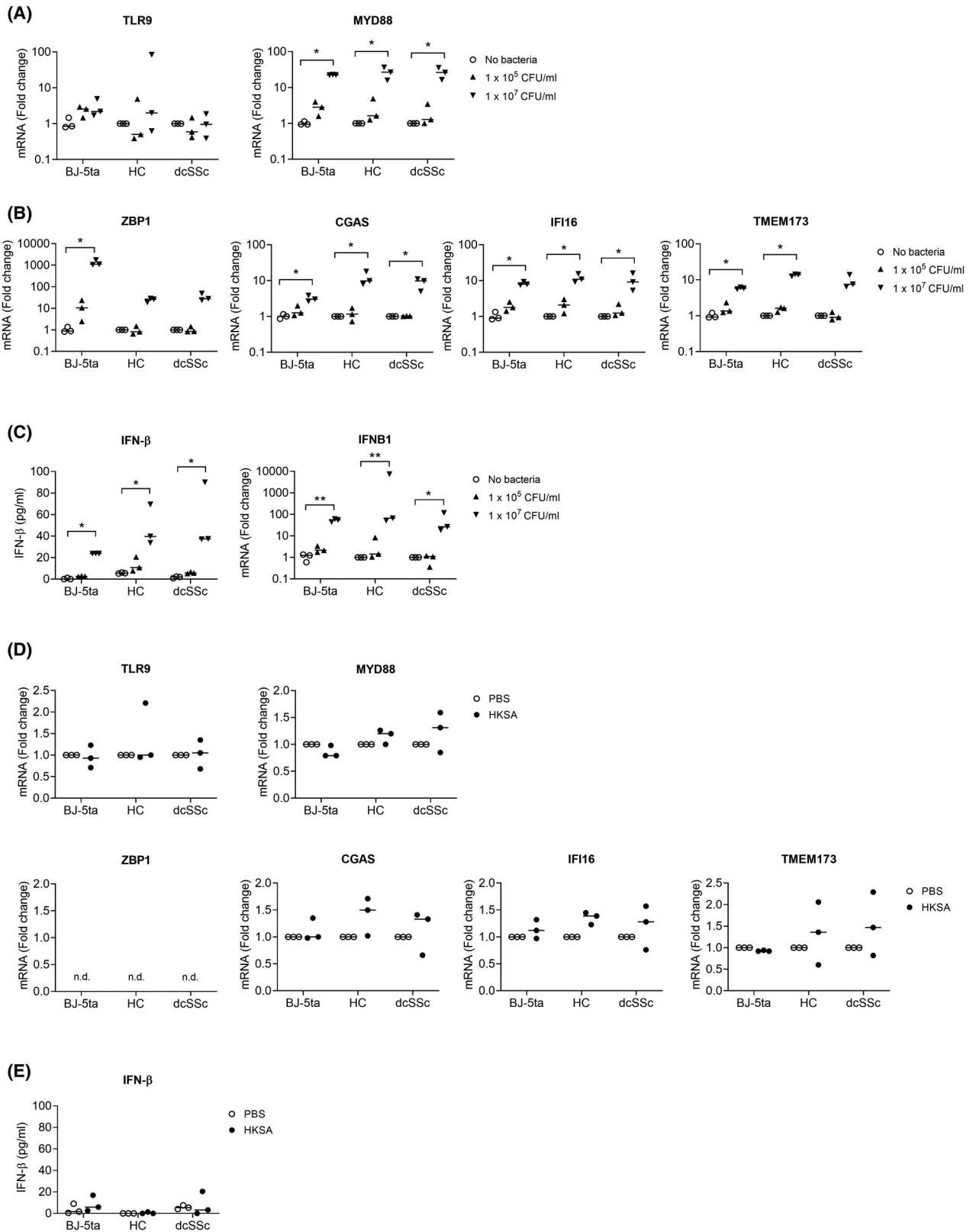
FIGURE 4 Gene expression of intracellular dsDNA sensors and their downstream mediators are upregulated upon SA exposure. A, The gene expression of TLR9 and its downstream mediator, MyD88 was evaluated at 24 h by qPCR analysis. B, The gene expression of STING (encoded by *TMEM173*) and its upstream DNA sensing molecules was evaluated at 24 h by qPCR analysis. C, IFN-β secretion was evaluated at 72 h by ELISA. The expression of IFN-β gene was evaluated at 24 h by qPCR. Bars show medians, n = 3 per group. *$P < .05$, **$P < .01$ (Kruskal-Wallis test followed by Dunn's multiple comparisons test). D and E, Human dermal fibroblasts were cultured with HKSA. D, The gene expression of intracellular DNA sensor genes was evaluated at 24 h by qPCR analysis. E, IFN-β secretion was evaluated at 72 h by ELISA. Bars show medians, n = 3 per group. The Wilcoxon-Mann-Whitney test was performed
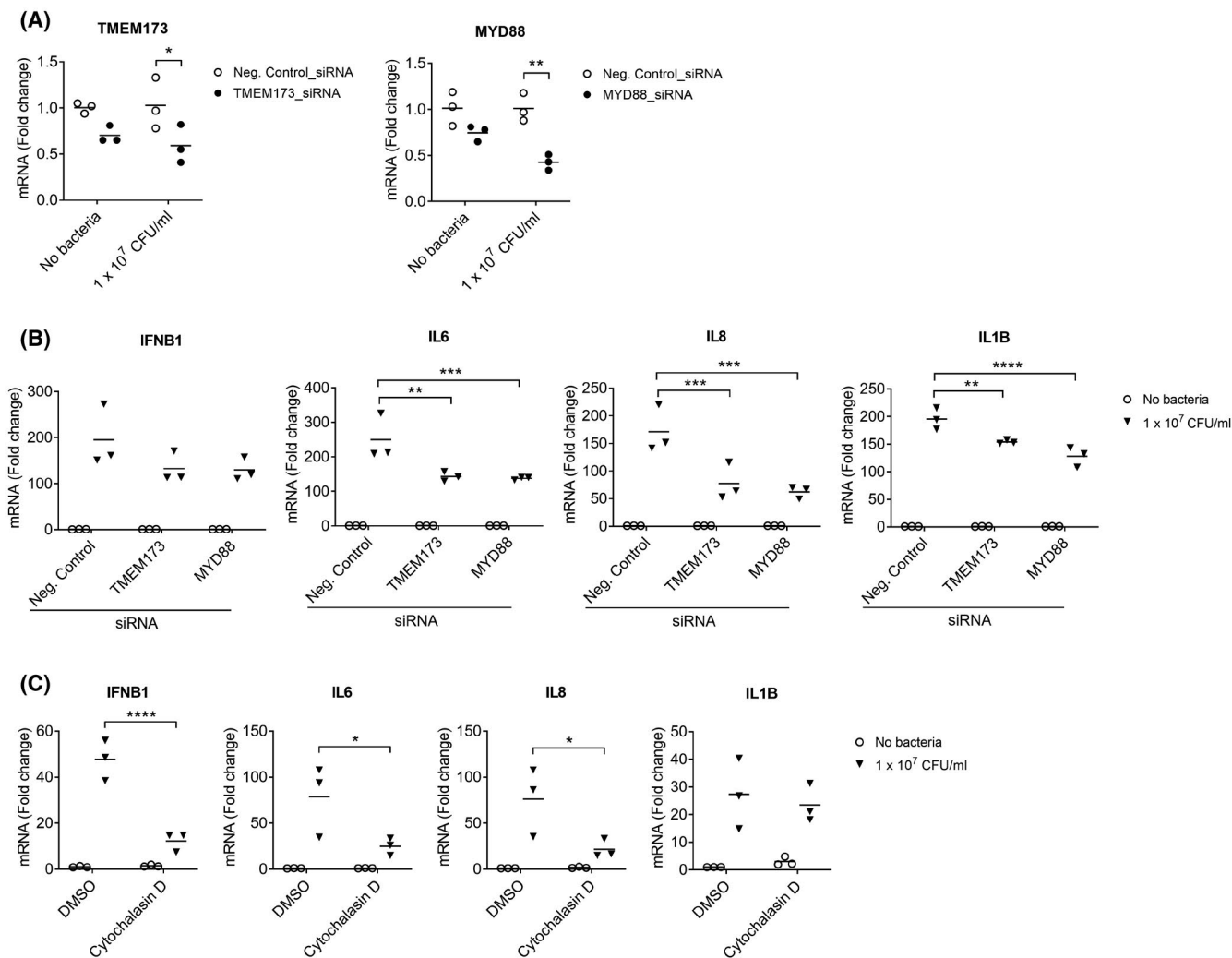
FIGURE 5 STING and MyD88 are crucial for the induction of IFN-β and pro-inflammatory mediators upon SA exposure. A, To present the efficacy of gene knockdown by siRNA, the gene expression data of TMEM173 and MYD88 in the samples are shown. B, BJ-5ta cells were treated with the indicated siRNA or negative control siRNA and then were co-cultured with SA. The gene expression of IFN-β, IL-6, IL-8, and IL-1β was evaluated at 24 h by qPCR analysis. C, BJ-5ta cells were treated with an endocytosis inhibitor, cytochalasin D (10 µg/mL) for 1 h before SA exposure and then were co-cultured with SA. The gene expression of IFN-β, IL-6, and IL-8, and IL-1β was evaluated at 24 h by qPCR analysis. Bars show means, n = 3 per group. *$P < .05$, **$P < .01$, ***$P < .001$, ****$P < .0001$ (Two-way ANOVA followed by Sidak's multiple comparisons test)

(bacterial) dsDNA sensor molecules, converging either on MyD88 or STING signaling pathways, might be involved in eliciting type I IFN responses, but also (NF-κB-mediated) pro-inflammatory cytokine release in dermal fibroblasts. The TLR9-MyD88 signaling pathway was thought to be key for the type I IFN production by bacterial dsDNA.[31] However, recent studies additionally identified STING as a major player in TLR-independent intracellular DNA sensing. A recent study provided evidence that in murine bone marrow-derived macrophages and the human macrophage cell line, THP-1, SA activated either STING (live SA) or TLR (dead SA) signaling pathways.[37] In our experiments using dermal fibroblasts, in contrast to live SA, HKSA had only negligible effects on both pathways and their downstream cytokines suggesting that TLR2 is not involved in these responses. The

internalization of HKSA was much less pronounced than that of live SA as assessed by confocal microscopic analyses (Figure 3B, Figures S7 and S8). Given that bacterial internalization was important for the robust expression of IL-6, IL-8, and IFN-β upon live SA exposure (Figure 5C), the reduced internalization of HKSA could be one of the reasons why HKSA did not induced inflammatory responses. Another possible reason is *vita*-PAMPs, through which the innate immune system can differentiate between live and dead microorganisms.[43] Cyclic-di-adenosine monophosphate (c-di-AMP) has been identified as one of the *vita*-PAMPs, which is a second messenger produced by Gram-positive bacteria.[44] c-di-AMP is known as a STING agonist.[45] Therefore, it is suggested that only live SA but not HKSA could induce IL-6, IL-8, and IFN-β through internalization and subsequent
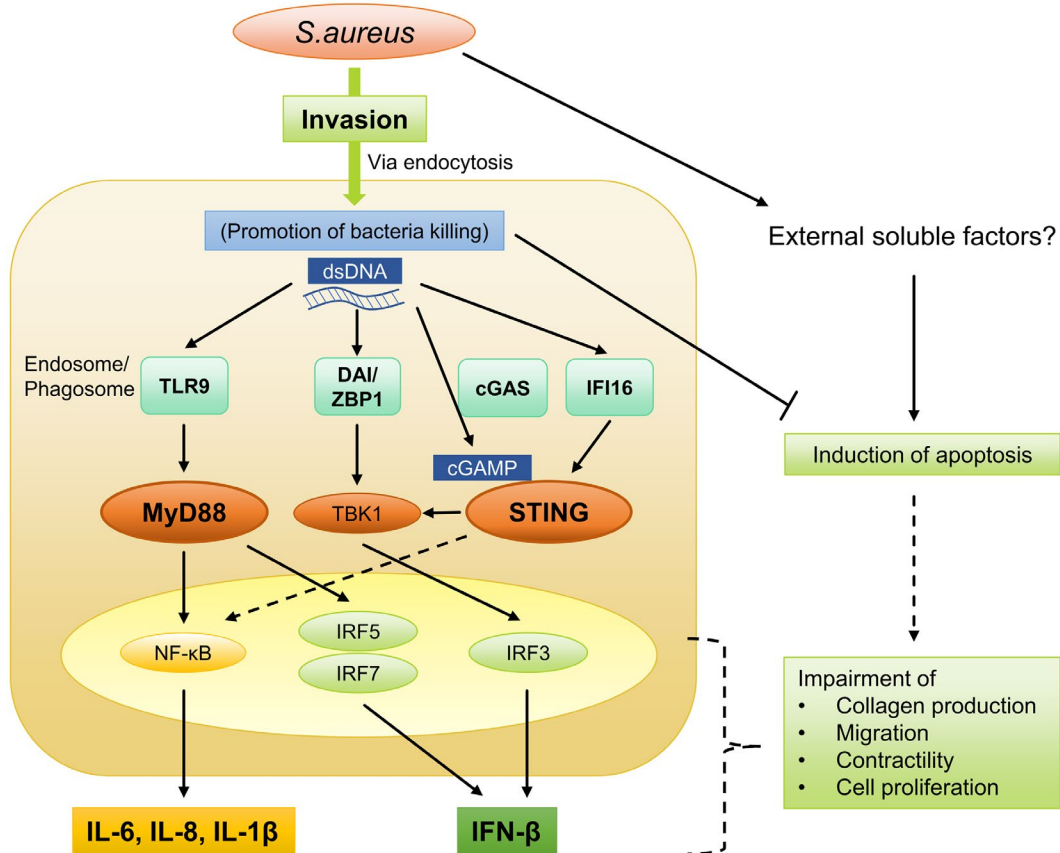
FIGURE 6 SA-fibroblast interactions in the context of tissue repair. Invasion of dermal fibroblasts by SA with activation of the STING and TLR9-MyD88 pathways is a key element in the impairment of tissue repair responses

activation of STING-pathway. Although in our experiments, bacterial invasion and dsDNA sensing seemed to relay the major effects, we cannot exclude that to some extent host dsDNA upon cell death of fibroblasts might have contributed to the activation of the STING pathway.[9]

In this proof of concept study, we intentionally made use of a "simplified" 2D cell culture system to be able to (a) identify SA-induced fibroblast responses with relevance for wound healing processes and (b) start to delineate involved signaling pathways. Although this in vitro 2D setting does not cover the real-life complexity of cell-cell- and cell-matrix interactions occurring in human dermal tissue repair, nor do most available animal models. Rodent models do not mirror the human situation of wound repair due to substantial differences in skin anatomy and (patho-) physiology.[46] Thus, ultimately, the use of a human 3D skin equivalent[3] for wound healing studies might be warranted to (a) further confirm our results and (b) allow to test therapeutic options with good transferability.

In conclusion, our study suggests that SA-induced alterations of dermal fibroblast responses might contribute to the chronicity and recurrence of dermal wounds. Although further studies are required, our results are in line with previous studies suggesting that targeting intracellular DNA sensing pathways[47] could represent a novel therapeutic approach for (SA-infected) non-healing wounds, which are being increasingly recognized as a health concern of epidemic proportions.[2]

CONFLICT OF INTERESTS

M. Yokota, M. Kassier, N. Häffner, F. Brennecke, M. Brunner, J. Schniering, S. Mairpady Shampath, E. Marques Maggio, and A. S. Zinkernagel have no competing interests to declare. O. Distler had consultancy relationships with Actelion, AnaMar, Bayer, Boehringer Ingelheim, Catenion, CSL Behring, ChemomAb, Roche, GSK, Inventiva, Italfarmaco, Lilly, medac, Medscape, Mitsubishi Tanabe Pharma, MSD, Novartis, Pfizer, Sanofi, and UCB in the area of potential treatments of scleroderma and its complications. Additionally, O.

AUTHOR CONTRIBUTIONS

M. Yokota made substantial contributions to the conception of the study and the acquisition, analysis and the interpretation of data and was involved in drafting and revising the manuscript. M. Kassier, N. Häffner, S. Mairpady Shampath, F. Brennecke, M. Brunner, E. Marques Maggio, and J. Schniering were centrally involved in the acquisition and analysis of data and in revising the manuscript. O. Distler and A.S. Zinkernagel made contributions to the conception and design of the study, the interpretation of the data and the revision of the manuscript. B. Maurer made substantial contributions to conception and design of the study and was centrally involved in the acquisition, analysis and interpretation of data and in drafting and revising the manuscript. All authors have given final approval of the version to be published.

DATA AVAILABILITY STATEMENT

All data are presented either in the main manuscript or in the data supplement.

REFERENCES

1. Edwards R, Harding KG. Bacteria and wound healing. *Curr Opin Infect Dis*. 2004;17:91-96.
2. Sen CK, Gordillo GM, Roy S, et al. Human skin wounds: a major and snowballing threat to public health and the economy. *Wound Repair Regen*. 2009;17:763-771.
3. Eming SA, Martin P, Tomic-Canic M. Wound repair and regeneration: mechanisms, signaling, and translation. *Sci Transl Med*. 2014;6:265sr266.
4. Wirz EG, Jaeger VK, Allanore Y, et al. Incidence and predictors of cutaneous manifestations during the early course of systemic sclerosis: a 10-year longitudinal study from the EUSTAR database. *Ann Rheum Dis*. 2016;75:1285-1292.
5. Denton CP, Krieg T, Guillevin L, et al. Demographic, clinical and antibody characteristics of patients with digital ulcers in systemic sclerosis: data from the DUO Registry. *Ann Rheum Dis*. 2012;71:718-721.
6. Gurtner GC, Werner S, Barrandon Y, Longaker MT. Wound repair and regeneration. *Nature*. 2008;453:314-321.
7. Scales BS, Huffnagle GB. The microbiome in wound repair and tissue fibrosis. *J Pathol*. 2013;229:323-331.
8. Giuggioli D, Manfredi A, Lumetti F, Colaci M, Ferri C. Scleroderma skin ulcers definition, classification and treatment strategies our experience and review of the literature. *Autoimmun Rev*. 2018;17:155-164.
9. Horn J, Stelzner K, Rudel T, Fraunholz M. Inside job: *Staphylococcus aureus* host-pathogen interactions. *Int J Med Microbiol*. 2018;308:607-624.
10. Giuggioli D, Manfredi A, Colaci M, Lumetti F, Ferri C. Scleroderma digital ulcers complicated by infection with fecal pathogens. *Arthritis Care Res*. 2012;64:295-297.
11. Giuggioli D, Manfredi A, Colaci M, Lumetti F, Ferri C. Osteomyelitis complicating scleroderma digital ulcers. *Clin Rheumatol*. 2013;32:623-627.
12. Lowy FD. *Staphylococcus aureus* infections. *N Engl J Med*. 1998;339:520-532.
13. Zhang X, Hu X, Rao X. Apoptosis induced by *Staphylococcus aureus* toxins. *Microbiol Res*. 2017;205:19-24.
14. Grice EA, Segre JA. Interaction of the microbiome with the innate immune response in chronic wounds. *Adv Exp Med Biol*. 2012;946:55-68.
15. Strobel M, Pfortner H, Tuchscherr L, et al. Post-invasion events after infection with *Staphylococcus aureus* are strongly dependent on both the host cell type and the infecting *S. aureus* strain. *Clin Microbiol Infect*. 2016;22:799-809.
16. Leimer N, Rachmuhl C, Palheiros Marques M, et al. Nonstable *Staphylococcus aureus* small-colony variants are induced by low pH and sensitized to antimicrobial therapy by phagolysosomal alkalinization. *J Infect Dis*. 2016;213:305-313.
17. Maurer B, Stanczyk J, Jungel A, et al. MicroRNA-29, a key regulator of collagen expression in systemic sclerosis. *Arthritis Rheum*. 2010;62:1733-1743.
18. Seidl K, Zinkernagel AS. The MTT assay is a rapid and reliable quantitative method to assess *Staphylococcus aureus* induced endothelial cell damage. *J Microbiol Methods*. 2013;92:307-309.
19. Bettenworth D, Lenz P, Krausewitz P, et al. Quantitative stain-free and continuous multimodal monitoring of wound healing in vitro with digital holographic microscopy. *PLoS One*. 2014;9:e107317.
20. Quiblier C, Seidl K, Roschitzki B, Zinkernagel AS, Berger-Bachi B, Senn MM. Secretome analysis defines the major role of SecDF in *Staphylococcus aureus* virulence. *PLoS One*. 2013;8:e63513.
21. Luria SE. A test for penicillin sensitivity and resistance in Staphylococcus. *Proc Soc Exp Biol Med*. 1946;61:46-51.
22. Beutler BA. TLRs and innate immunity. *Blood*. 2009;113:1399-1407.
23. Loffler B, Tuchscherr L, Niemann S, Peters G. *Staphylococcus aureus* persistence in non-professional phagocytes. *Int J Med Microbiol*. 2014;304:170-176.
24. Sinha B, Fraunholz M. *Staphylococcus aureus* host cell invasion and post-invasion events. *Int J Med Microbiol*. 2010;300:170-175.
25. Agerer F, Lux S, Michel A, Rohde M, Ohlsen K, Hauck CR. Cellular invasion by *Staphylococcus aureus* reveals a functional link between focal adhesion kinase and cortactin in integrin-mediated internalisation. *J Cell Sci*. 2005;118:2189-2200.
26. Sayedyahossein S, Xu SX, Rudkouskaya A, McGavin MJ, McCormick JK, Dagnino L. *Staphylococcus aureus* keratinocyte invasion is mediated by integrin-linked kinase and Rac1. *FASEB J*. 2015;29:711-723.
27. Josse J, Laurent F, Diot A. Staphylococcal Adhesion and Host Cell Invasion: Fibronectin-Binding and Other Mechanisms. *Front Microbiol*. 2017;8:2433.
28. Surewaard BG, Deniset JF, Zemp FJ, et al. Identification and treatment of the *Staphylococcus aureus* reservoir in vivo. *J Exp Med*. 2016;213:1141-1151.
29. Fraunholz M, Sinha B. Intracellular *Staphylococcus aureus*: live-in and let die. *Front Cell Infect Microbiol*. 2012;2:43.

30. Amano A, Nakagawa I, Yoshimori T. Autophagy in innate immunity against intracellular bacteria. *J Biochem*. 2006;140:161-166.

31. Parker D, Prince A. *Staphylococcus aureus* induces type I IFN signaling in dendritic cells via TLR9. *J Immunol*. 2012;189:4040-4046.

32. Bergstrom B, Aune MH, Awuh JA, et al. TLR8 Senses *Staphylococcus aureus* RNA in Human Primary Monocytes and Macrophages and Induces IFN-beta Production via a TAK1-IKKbeta-IRF5 Signaling Pathway. *J Immunol*. 2015;195:1100-1111.

33. Hruz P, Zinkernagel AS, Jenikova G, et al. NOD2 contributes to cutaneous defense against *Staphylococcus aureus* through alpha-toxin-dependent innate immune activation. *Proc Natl Acad Sci U S A*. 2009;106:12873-12878.

34. Munoz-Planillo R, Franchi L, Miller LS, Nunez G. A critical role for hemolysins and bacterial lipoproteins in *Staphylococcus aureus*-induced activation of the Nlrp3 inflammasome. *J Immunol*. 2009;183:3942-3948.

35. Hanamsagar R, Aldrich A, Kielian T. Critical role for the AIM2 inflammasome during acute CNS bacterial infection. *J Neurochem*. 2014;129:704-711.

36. Guarda G, Braun M, Staehli F, et al. Type I interferon inhibits interleukin-1 production and inflammasome activation. *Immunity*. 2011;34:213-223.

37. Scumpia PO, Botten GA, Norman JS, et al. Opposing roles of Toll-like receptor and cytosolic DNA-STING signaling pathways for *Staphylococcus aureus* cutaneous host defense. *PLoS Pathog*. 2017;13:e1006496.

38. Pei J, Zhang Y, Luo Q, et al. STAT3 inhibition enhances CDN-induced STING signaling and antitumor immunity. *Cancer Lett*. 2019;450:110-122.

39. Rahim K, Saleha S, Zhu X, Huo L, Basit A, Franco OL. Bacterial contribution in chronicity of wounds. *Microb Ecol*. 2017;73:710-721.

40. Tuchscherr L, Medina E, Hussain M, et al. *Staphylococcus aureus* phenotype switching: an effective bacterial strategy to escape host immune response and establish a chronic infection. *EMBO Mol Med*. 2011;3:129-141.

41. Smith RS, Smith TJ, Blieden TM, Phipps RP. Fibroblasts as sentinel cells - synthesis of chemokines and regulation of inflammation. *Am J Pathol*. 1997;151:317-322.

42. Xia Y, Pauza ME, Feng L, Lo D. RelB regulation of chemokine expression modulates local inflammation. *Am J Pathol*. 1997;151:375-387.

43. Sander LE, Davis MJ, Boekschoten MV, et al. Detection of prokaryotic mRNA signifies microbial viability and promotes immunity. *Nature*. 2011;474:385-389.

44. Moretti J, Roy S, Bozec D, et al. STING senses microbial viability to orchestrate stress-mediated autophagy of the endoplasmic reticulum. *Cell*. 2017;171:809-823.e813.

45. Burdette DL, Monroe KM, Sotelo-Troha K, et al. STING is a direct innate immune sensor of cyclic di-GMP. *Nature*. 2011;478:515-518.

46. Nunan R, Harding KG, Martin P. Clinical challenges of chronic wounds: searching for an optimal animal model to recapitulate their complexity. *Dis Model Mech*. 2014;7:1205-1213.

47. Haag SM, Gulen MF, Reymond L, et al. Targeting STING with covalent small-molecule inhibitors. *Nature*. 2018;559:269-273.

SUPPORTING INFORMATION

Additional supporting information may be found online in the Supporting Information section.

How to cite this article: Yokota M, Häffner N, Kassier M, et al. *Staphylococcus aureus* impairs dermal fibroblast functions with deleterious effects on wound healing. *The FASEB Journal*. 2021;35:e21695. https://doi.org/10.1096/fj.201902836R